

# Fabrication of Low-to-Zero Shrinkage Reaction-Bonded Mullite Composites

Dietmar Holz,<sup>a</sup> Sonja Pagel,<sup>a</sup> Chris Bowen,<sup>b</sup> Suxing Wu<sup>c</sup> & Nils Claussen<sup>d</sup>

<sup>a</sup>Philips WEB, 22419 Hamburg, Germany

<sup>b</sup>University of Leeds, School of Materials, Leeds, UK

<sup>c</sup>Lehigh University, Materials Research Center, Bethlehem, USA

<sup>d</sup>Technische Universität Hamburg-Harburg, Advanced Ceramics Group, 21071 Hamburg, Germany

(Accepted 22 July 1995)

## Abstract

*The technology of reaction bonding  $Al_2O_3$  (RBAO) can be modified by the use of Si-containing additives to yield low-to-zero shrinkage mullite composites. In the present work, SiC particles were added to the  $Al/Al_2O_3$  precursor mixture. During air heat-treatment, first Al oxidizes to  $Al_2O_3$  at 300–900°C, thereafter SiC converts to  $SiO_2$  (900–1200°C). Both phases form mullite ( $3Al_2O_3 \cdot SiO_2$ ) at temperatures >1400°C. Depending on the hold time at 900–1200°C, the extent of SiC oxidation, hence the ratio of mullite to dispersed SiC can be controlled. Since both oxidation reactions and the mullitization are associated with volume expansions, the sintering shrinkage can either be fully or partially compensated for. The process parameters amount of Al and SiC, green density and degree of SiC oxidation can be utilized to fabricate low-to-zero shrinkage mullite composites.*

## 1 Introduction

In recent years, the development of high-strength mullite for engineering and electronic applications has become a new area of ceramic research. This is due to many advantageous properties like high melting point, good creep resistance, low thermal expansion, low dielectric constant, and good corrosion resistance.<sup>1</sup> However, the mechanical properties of plain mullite are low (bending strength:  $\approx 250$  MPa, fracture toughness:  $\approx 2.5$  MPa m<sup>1/2</sup>) when compared to other ceramics.<sup>2</sup> Therefore, several mullite composites have been fabricated to improve the mechanical properties, e.g. by adding  $ZrO_2$  as well as platelets, whisker, or fibers.<sup>3–7</sup> The

fabrication of these improved mullite composites often requires new processing routes, such as sol-gel techniques combined with hot pressing, which limits the shape and size of the product and reduces the economy of the process.

The Reaction Bonding of Aluminum Oxide (RBAO) technology,<sup>8–10</sup> provides a new processing route to fabricate low-to-zero shrinkage high-strength mullite composites.<sup>11–13</sup> The plain RBAO process, which results in a product consisting only of  $Al_2O_3$ , starts from intensively milled  $Al/Al_2O_3$  precursor powder mixtures. Heating powder compacts in oxidizing atmosphere (usually air) up to temperatures of  $\sim 900^\circ\text{C}$  results in complete oxidation of Al to  $Al_2O_3$ . Due to very small 'new'  $Al_2O_3$  crystallites, sintering starts at  $\sim 1100^\circ\text{C}$ . The Al oxidation results in a 28% volume expansion partially compensating for the sintering shrinkage. Therefore, low shrinkage (5–15%)  $Al_2O_3$  ceramics are readily fabricated. In order to further reduce the shrinkage even to zero, the RBAO process can be modified in various ways by incorporating other metal or ceramic additives that exhibit volume expansions on oxidation which further compensate for the sintering shrinkage.

In this work, SiC additions are utilized to form mullite ceramics. Because of the large volume expansion associated with both the oxidation of SiC to  $SiO_2$  (108%) and with the mullite ( $3Al_2O_3 \cdot SiO_2$ ) formation (4.2%), the sintering shrinkage is effectively compensated. In this respect, 26 vol.% in the precursor powder composition is necessary to fabricate pure mullite.<sup>11</sup> Therefore, the heat treatment should be set ensuring complete oxidation of SiC. If the heat treatment is selected such that the SiC particles are not completely oxidized, various mullite/ $Al_2O_3$ /SiC composites result. The aim of this paper is to describe and to discuss the formation of low-to-zero shrinkage mullite composites obtained by the RBAO technology.

2 Experimental

Powder compositions and sources of raw materials used are listed in Table 1. The notations for the compositions contain the SiC content in vol.% in the precursor composition and a small letter defining the SiC particle size (c for coarse and f for fine). The powder mixtures were attrition-milled in acetone for 7 h with TZP (3Y-ZrO<sub>2</sub>) milling media. The amount of ZrO<sub>2</sub> introduced into the powder was estimated from qualitative phase analyses of the reaction-bonded samples. After milling, the powder was dried and sieved with a 200 μm mesh. Green bodies were produced by uniaxial pressing at 50 MPa followed by cold isostatic compaction (CIP) at pressures of 300 and 900 MPa. Oxidation and sintering was carried out in a box furnace in air using the heating cycle shown in Fig. 1. At 1150°C, a dwell time of 15 h (coarse SiC) and 10 h (fine SiC) was selected to ensure complete oxidation of SiC. This temperature was chosen because sintering is not yet significant, hence the powder compacts still contain open porosity. Therefore, the carbon monoxide produced by the SiC oxidation can diffuse outwards. Sintering was carried out at 1550°C for 1 h. The density of the final products was measured by the Archimedes method. Reaction products were identified by X-ray diffraction (XRD). Qualitative phase compositions were determined by Rietveld analysis. Microstructures were investigated by transmission electron microscopy (TEM).

Table 1. RBAO precursor powder compositions

|   | SC30c           | SC30f           | SC45f           |
|---|-----------------|-----------------|-----------------|
| <sup>1</sup> Al                             | 40              | 40              | 40              |
| <sup>2</sup> Al <sub>2</sub> O <sub>3</sub> | 30              | 30              | 15              |
| SiC   | <sup>3</sup> 30 | <sup>4</sup> 30 | <sup>4</sup> 45 |

<sup>1</sup>Alcan 105, < 50 μm, globular, Alcan International, Canada.  
<sup>2</sup>Ceralox HPA-0.5, ≈ 0.8 μm, Condea Chemie GmbH, Brunsbüttel, Germany.  
<sup>3</sup>F1000, 2.5–3.5 μm, Norton AS, Lillesand, Norway.  
<sup>4</sup>Ultra-fine, 0.27 μm, Ibiden Co., Ogaki, Japan.

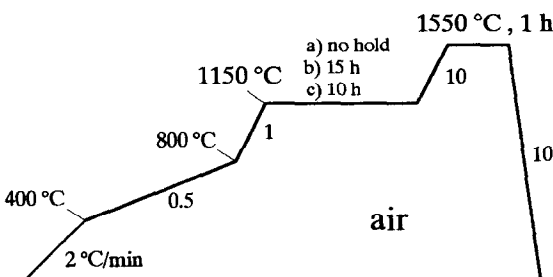


Fig. 1. Heat treatment cycles: (a) without and (b, c) with oxidation holds for SiC.

3 Results and Discussion

3.1 Phase development

The XRD diagrams (Fig. 2) of composition SC30c at 1150°C without and with 15 h hold show that, for both temperature cycles, all Al has been completely oxidized, and that a large amount of ZrO<sub>2</sub> is introduced (12–15%) during milling. It originates from wear debris of the TZP balls and discs. Composition SC30f (fine SiC) contains somewhat less ZrO<sub>2</sub> (~10%) which is due to the reduced aggressiveness of the smaller SiC particles. When using coarse SiC, it is impossible to get complete oxidation, even after 15 h hold, while with finer SiC (SC30f), even 10 h at 1150°C are sufficient. The oxidation product is amorphous SiO<sub>2</sub> not detectable by XRD. It has been shown previously<sup>11</sup> that crystalline SiO<sub>2</sub> (α-cristobalite) does not form until ~1200°C.

Phase compositions of samples SC30c and SC30f after sintering at 1550°C for 1 h are shown in Fig. 3. Sample SC30c without holding at 1150°C (SC30c1550/0, left bar) consists of mullite/Al<sub>2</sub>O<sub>3</sub>/SiC/

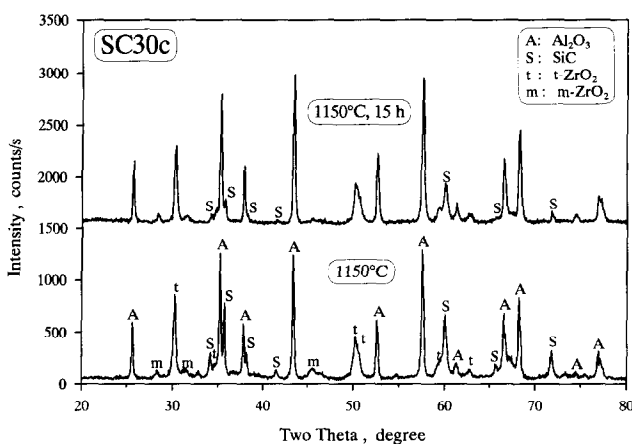


Fig. 2. XRD diagrams of sample SC30c without and with hold for 15 h at 1150°C.

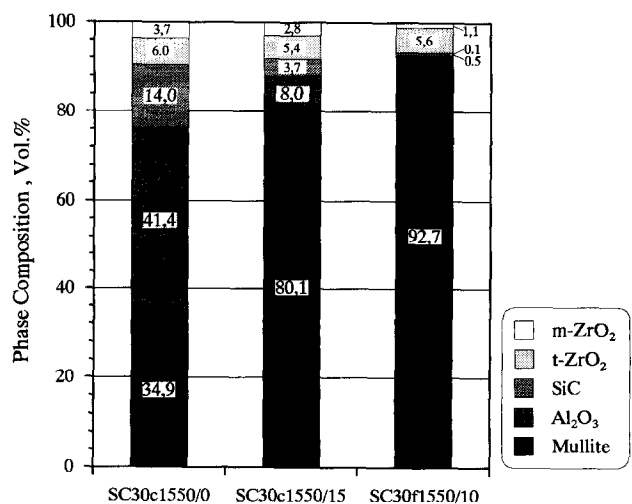


Fig. 3. Phase compositions of samples SC30c and SC30f after sintering at 1550°C for 1 h.

t-ZrO<sub>2</sub>/m-ZrO<sub>2</sub> (34.9/41.4/14.0/6.0/3.7 vol.%). After holding at 1150°C for 15 h (SC30c1550/15) before sintering, the sample still contains mullite/Al<sub>2</sub>O<sub>3</sub>/SiC/t-ZrO<sub>2</sub>/m-ZrO<sub>2</sub> (80.1/8.0/3.7/5.4/2.8 vol.%). Due to the higher degree of SiC oxidation though, the amount of mullite is strongly increased and correspondingly the content of Al<sub>2</sub>O<sub>3</sub> and SiC is lower. When coarse SiC is used neither dwell time nor heat-up time to the sintering temperature (heating rate is 10°C/min) are sufficient to allow complete SiC oxidation. However, sample SC30f after holding at 1150°C for 10 h before sintering (SC30f1550/10, Fig. 3 right bar) consists mainly of mullite and ZrO<sub>2</sub> (92.7/6.7 vol.%). Only traces of Al<sub>2</sub>O<sub>3</sub> and SiC are left (<0.5 / <0.1 vol.%).

It is interesting to note that, at temperatures >1400°C in air, samples with non-completely oxidized SiC always have a white outer layer consisting of mullite and Zircon (ZrSiO<sub>4</sub>). This effect is attributed to preferred densification in the surface region due to oxidation of SiC and mullite formation. These reactions are associated with a volume increase enhancing surface layer densification and thus hindering oxygen diffusion inwards thereby preventing further oxidation in the interior. The formation of Zircon can be explained by an excess of SiC leading to a reaction of SiO<sub>2</sub> with ZrO<sub>2</sub>. With progressing densification, the trapped gas inside of the sample, due to further SiC oxidation, diffuses outwards resulting in a higher porosity of the outer layer which remains even after sintering. Prevention of this layer can be achieved by initially oxidizing the SiC and Al in air and sintering the body in an inert atmosphere.

### 3.2 Microstructural development

The TEM micrograph (Fig. 4) of sample SC30c after holding at 1150°C for 15 h demonstrates that, when using coarse SiC particles, the heat treatment used is not sufficient for complete oxidation of all SiC particles. For this heating schedule, the critical SiC particle size after milling for complete oxidation is ~0.3–0.4 µm. The amorphous oxide layer thickness around SiC particles larger than this critical size is ~0.15–0.2 µm.

Figure 5 shows microstructures of samples SC30f after sintering at 1550°C for 1 h (a) without and (b) with hold at 1150°C for 10 h. The microstructure of the sample without hold (Fig. 5(a)) consists of mullite, Al<sub>2</sub>O<sub>3</sub>, SiC, and ZrO<sub>2</sub> (cf. Section 3.1). The grain sizes of all phases are ≤ 1 µm. Mullite and Al<sub>2</sub>O<sub>3</sub> grains cannot be distinguished optically, only by EDX. SiC as well as ZrO<sub>2</sub> particles are mostly located at mullite or Al<sub>2</sub>O<sub>3</sub> grain boundaries. SiC show the typical polytype structure. Some small SiC particles are located within the mullite grains. In contrast to XRD

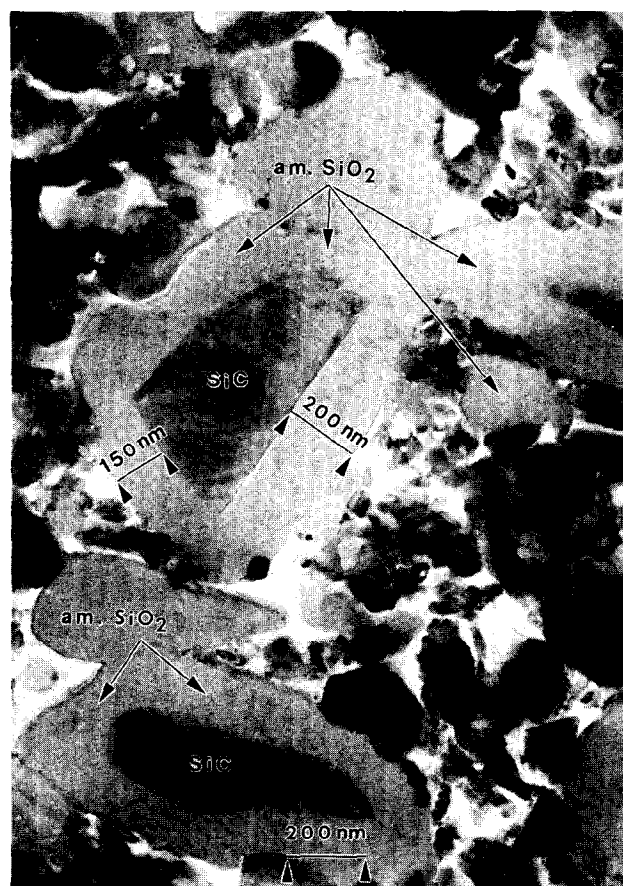


Fig. 4. TEM micrograph demonstrating the effect of SiC oxidation at 1150°C for 15 h.

results, ZrO<sub>2</sub> is in monoclinic crystal symmetry. The tetragonal-to-monoclinic phase transformation is attributed to TEM sample preparation.

The microstructure of SC30f in Fig. 5(b) after sintering at 1550°C with hold at 1150°C for 10 h (complete SiC oxidation) is characterized by a dense and homogeneous mullite matrix with ZrO<sub>2</sub> dispersions at grain boundaries and Al<sub>2</sub>O<sub>3</sub> particles inside mullite grains. Some tiny SiC particles are also found within mullite grains. The survival of these SiC particles can be explained by reduced oxygen access in the final state of densification. Consequently, also some small Al<sub>2</sub>O<sub>3</sub> particles survive embedded in mullite during grain growth. The density of this mullite/ZrO<sub>2</sub> sample is somewhat higher (96%) than that shown in Fig. 5(a) (94.5%). This is due to the increased SiC content which is known to hinder densification of Al<sub>2</sub>O<sub>3</sub>.<sup>14,15</sup>

### 3.3 Zero-shrinkage conditions

The shrinkage calculation of mullite composites requires the knowledge of: (a) the fraction of Al oxidized during milling (*f*); (b) the fraction of ZrO<sub>2</sub> introduced by milling wear (*V*<sub>ZrO<sub>2</sub></sub>); (c) the degree of SiC oxidation during reaction bonding (*Ψ*) and (d) green (*ρ*<sub>o</sub>) and final density (*ρ*). The

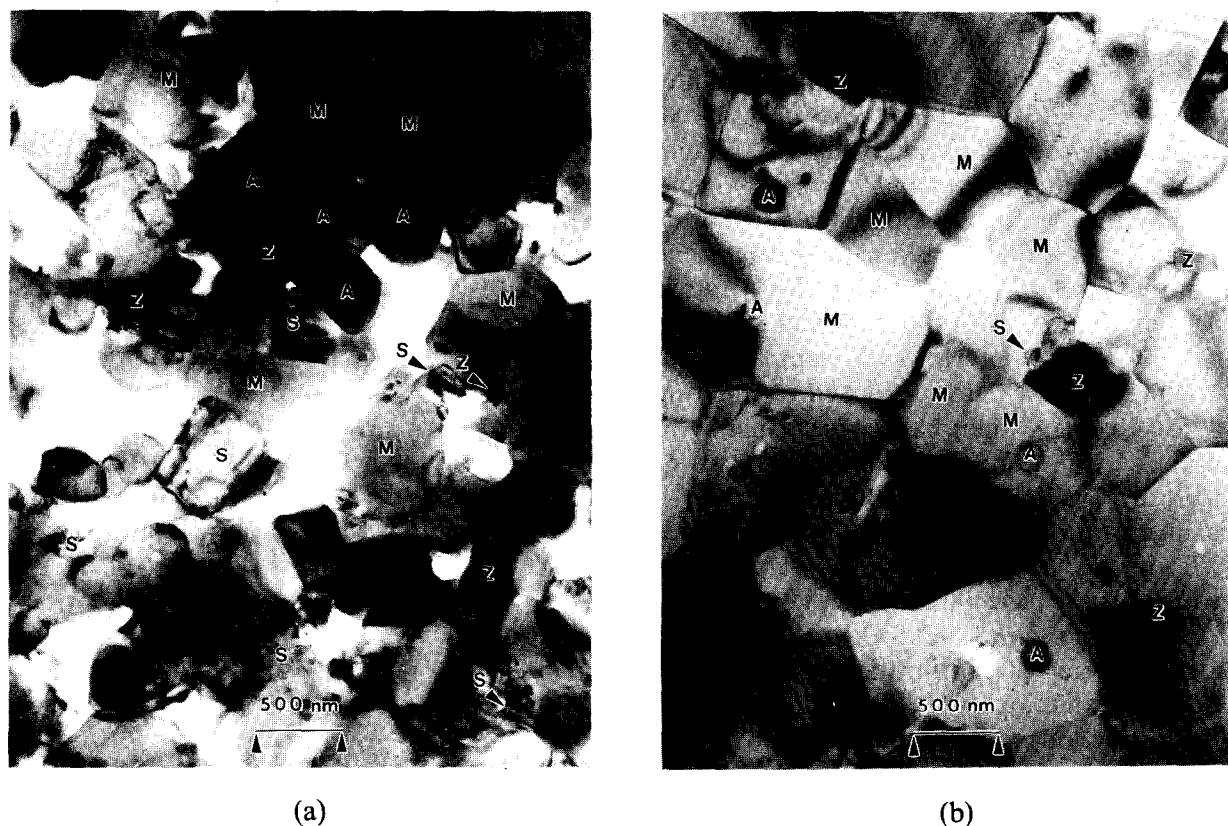


Fig. 5. TEM micrographs showing composition SC30f after sintering at 1550°C for 1 h: (a) without and (b) with hold at 1150°C for 10 h (M: Mullite, A: Al<sub>2</sub>O<sub>3</sub>, S: SiC, Z: ZrO<sub>2</sub>).

determination of  $f$  has been described elsewhere<sup>9</sup> and can be done by quantitative X-ray or thermogravimetric analyses. Typical values for  $f$  are 0.3–0.5.  $V_{\text{ZrO}_2}$  can be determined by different methods: (a) XRD analysis of the milled powder (difficult because of the amorphous Al<sub>2</sub>O<sub>3</sub>); (b) weighing the milling discs and balls before and after milling (not very accurate), and (c) quantitative XRD phase analysis of reaction-bonded bodies. Method (c), e.g. Rietveld analysis, enables the exact determination of phase composition after reaction bonding, however, phase composition depends strongly on the degree of SiC oxidation. Therefore, exact calculation of  $V_{\text{ZrO}_2}$  requires the determination of the ZrO<sub>2</sub> content of a sample with completely oxidized SiC ( $\psi = 1$ ).  $V_{\text{ZrO}_2}$  can then be calculated considering the ZrO<sub>2</sub> volume fraction in the final composition ( $V_{\text{ZrO}_2}^{\#}$ ) and the volume expansion during reaction bonding.<sup>10</sup>

$$V_{\text{ZrO}_2} = \frac{\left( \frac{1 + 0.28V_{\text{Al}} + 1.125V_{\text{SiC}}}{1 + 0.60fV_{\text{Al}}} \right) \cdot V_{\text{ZrO}_2}^{\#}}{1 - V_{\text{ZrO}_2}^{\#}} \quad (1)$$

Thereby, 0.28 and 1.125 are the volume expansions associated with the Al oxidation (0.28) and the combination of SiC oxidation (0.08) and mullite formation (0.042), and  $V_{\text{Al}}$  and  $V_{\text{SiC}}$  the respective volume fractions. 0.60 is the volume expansion

associated with the oxidation of Al to amorphous Al<sub>2</sub>O<sub>3</sub> (density ~3.2 g/cm<sup>3</sup>) during milling.<sup>10</sup>

Exact shrinkage calculations require the reevaluation of the true volume fractions of each phase after milling ( $V_i^*$ ). The true volume fraction is given by the ratio of volume fraction before milling ( $V_i$ ) to increased total volume after milling (formation of amorphous Al<sub>2</sub>O<sub>3</sub> and ZrO<sub>2</sub> wear debris).

$$V_i^* = \frac{V_i}{1 + 0.60fV_{\text{Al}} + V_{\text{ZrO}_2}} \quad (2)$$

Equation (2) also enables the differentiation between the volume fraction of Al left after milling ( $V_{\text{Al}}^*$ ) and the volume fraction of Al oxidized to amorphous Al<sub>2</sub>O<sub>3</sub> ( $V_{\text{amorph}}^*$ ). In this case,  $V_i$  for Al is equal to  $(1-f)V_{\text{Al}}$  and for amorphous Al<sub>2</sub>O<sub>3</sub> equal to  $1.60fV_{\text{Al}}$ , respectively. Generally speaking, the volume increase during reaction bonding due to oxidation of Al can be calculated either by considering  $V_{\text{Al}}$  and  $f$  (see also Ref. 10) or by the real volume fractions, as demonstrated in eqn (3). Thereby, -0.20 is the volume decrease associated with the phase transformation of amorphous Al<sub>2</sub>O<sub>3</sub> to  $\alpha$ -modification. However, in case when for shrinkage calculations also wear debris has to be considered always the real volume fractions have to be determined.

$$\frac{1 + 0.28V_{Al}}{1 + 0.60fV_{Al}} = 1 + 0.28V_{Al}^* + 0.20V_{amorph}^* \quad (3)$$

To determine the degree of SiC oxidation during reaction bonding ( $\psi$ ), the SiC phase content after reaction bonding ( $V_{SiC}^{\#}$ ) has to be measured, e.g. by Rietveld analysis.  $V_{SiC}^{\#}$  is also given by the volume ratio of non-oxidized SiC ( $(1-\psi)V_{SiC}^*$ ) to total volume after reaction bonding.

$$V_{SiC}^{\#} = \frac{(1-\psi)V_{SiC}^*}{1 + 0.28V_{Al}^* - 0.20V_{amorph}^* + 1.125\psi V_{SiC}^{\#}} \quad (4)$$

Rearranging eqn (4) gives:

$$\psi = \frac{1 - \frac{V_{SiC}^*}{V_{SiC}^{\#}} (1 + 0.28V_{Al}^* - 0.20V_{amorph}^*)}{1 + 1.125V_{SiC}^{\#}} \quad (5)$$

The shrinkage calculation also requires the knowledge of relative green ( $\rho_o$ ) and final ( $\rho$ ) density. Therefore, theoretical green and final density have to be calculated considering the true volume fractions. A modified equation predicting the total dimensional linear change,  $S$ , during reaction bonding of SiC-containing RBAO ceramics is then given by

$$S = \left[ (1 + 0.28V_{Al}^* - 0.20V_{amorph}^* + 1.125\psi V_{SiC}^{\#}) \frac{\rho_o}{\rho} \right]^{\frac{1}{3}} - 1 \quad (6)$$

Following eqn (6), the conditions for low-to-zero shrinkage are high Al and SiC contents, complete oxidation ( $\psi = 1$ ), low fraction of Al oxidized during milling ( $V_{amorph}^*$  small), and high green and

low final densities. In composition SC30, the Al and SiC content is given with 40 and 30 vol.% in the precursor powder. Calculations according to eqn (6) for low-to-zero shrinkage conditions assuming  $\psi = 1$  (complete SiC oxidation) and  $V_{ZrO_2}^{\#} = 10$  vol.% together with general trends mentioned before are given in Fig. 6. A low-to-zero shrinkage range can be defined for samples with 90% final density and  $f = 0$  as an upper limit and with 100% final density and  $f = 0.5$  as a lower limit. The dashed line represents samples with 100% final density and  $f = 0$ .

A green machined sample of composition SC30 was fabricated with a linear shrinkage of 0.6%, 96% TD final density, and a  $ZrO_2$  content of 6.7 vol.% (see Fig. 7). The green density was 68% TD (CIP pressure: 900 MPa),  $f \sim 0.3$ , and SiC completely oxidized. According to eqns (1) and (2), the phase composition in the powder mixture after milling has been calculated to be 23.7/16.2/25.2/25.2/19.7 vol.% (Al, amorphous  $Al_2O_3$ ,  $Al_2O_3$ , SiC, and  $ZrO_2$ ), respectively. Calculating the linear dimensional change according to eqn (6) and considering the true phase composition gives a shrinkage of 2.1% which is higher than the experimental value. This can be explained by an increased volume of the porous outer layer consisting of mullite and Zircon (see Section 3.1). Neglecting the change of phase composition due to  $ZrO_2$  wear debris gives a linear shrinkage of 1.4% which is similar to that considering  $V_{ZrO_2}^*$ . The calculated and experimentally determined shrinkage values are also presented in Fig. 6.

In order to reduce the required green density for zero-shrinkage behavior, SiC contents > 26 vol.% may be used to further increase the oxidation expansion. However, when more than 26 vol.% SiC is used, an excess of  $SiO_2$  remains. Therefore, the volume expansion due to SiC oxidation ( $\Delta V_{SiC}$ ) has to be modified considering the

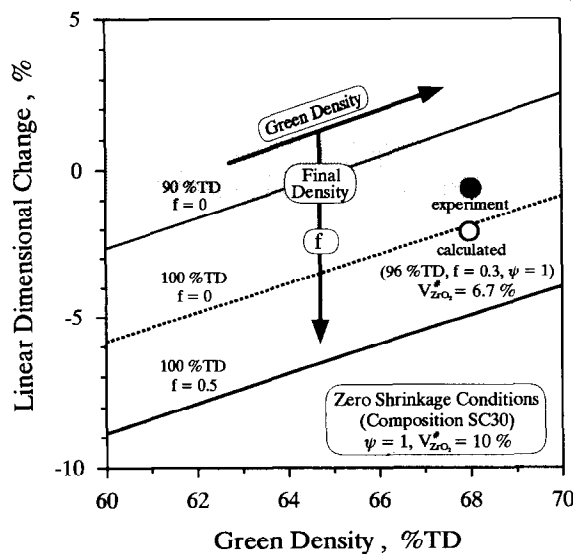


Fig. 6. Calculated linear dimensional change (according to eqn (1)) of composition SC30 for 90 and 100% final density. Experimental and calculated data points for composition SC30 (68 and 96% green and final density,  $f = 0.3$ ) are also given.

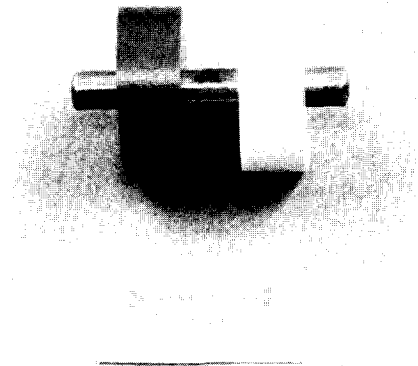


Fig. 7. Photograph demonstrating zero-shrinkage of a part made from composition SC30. The inner diameter of the green (dark) and reaction-bonded part (white) did not change.

amount of remaining  $\text{SiO}_2$ .  $\Delta V_{\text{SiC}}$  is then a combination of only SiC oxidation ( $\Delta V_{\text{SiC} \rightarrow \text{SiO}_2} = 1.08$ ) and SiC oxidation plus mullitization ( $\Delta V_{\text{SiC} \rightarrow \text{mullite}} = 1.125$ ). A composition consisting of 40/15/45 vol.% Al/ $\text{Al}_2\text{O}_3$ /SiC (SC45) was fabricated and a shrinkage of 1% (97% final density) was observed using a CIP pressure of only 300 MPa. The presence of  $\text{SiO}_2$  would possibly reduce the high temperature strength of the composite.

#### 4 Conclusions

- (1) The RBAO process can be modified by adding SiC to the precursor powder mixture to fabricate low-to-zero shrinkage mullite/ $\text{Al}_2\text{O}_3$ /SiC/ $\text{ZrO}_2$  composites. Attrition-milling of RBAO precursor powders is normally carried out with TZP balls and discs which introduces, when SiC is present, a substantial amount of  $\text{ZrO}_2$  wear debris into the mixture (10–15%).  $\text{ZrO}_2$  is not necessary for the RBAO process, however, it improves the microstructural development.<sup>8</sup>
- (2) The phase ratio of mullite to SiC in the final composition can be varied by adjusting the degree of SiC oxidation.
- (3) The exact calculation of the linear dimensional change during reaction bonding requires the determination of the true volume fractions of each phase in the green and sintered state considering the fraction of Al oxidized during milling, the  $\text{ZrO}_2$  wear debris, and the degree of SiC oxidation.
- (4) To achieve zero shrinkage, high SiC contents (>26%), high green densities (>65%) and complete SiC oxidation are required. Therefore, small SiC powders (<1  $\mu\text{m}$ ) and intensive milling are recommended.
- (5) In order to reduce the required green density for zero shrinkage, SiC contents >30% should be used to further increase the oxidation expansion. However, when >26% SiC is used, excess  $\text{SiO}_2$  remain in the body.
- (6) At temperatures >1400°C, a white porous outer layer consisting of mullite and Zircon ( $\text{ZrSiO}_4$ ) is produced. Prevention of this layer can be achieved by initially oxidizing the SiC and Al in air and sintering the body in an inert atmosphere.
- (7) Reaction-bonded mullite/ $\text{Al}_2\text{O}_3$ /SiC/ $\text{ZrO}_2$  com-

posites exhibit superior mechanical properties. These results are published elsewhere.<sup>12</sup>

#### Acknowledgements

The authors thank Deutsche Forschungsgemeinschaft (DFG) for financial support under contracts No. Cl 52/12-2 and Cl 52/23-1. Thanks are also due to D. Thiele for Rietveld analyses.

#### References

1. Schneider, H., Okada, K. & Pask, J. A., *Mullite and Mullite Ceramics*, John Wiley & Sons, Chichester, 1994.
2. Kanzaki, S., Tabata, H., Kumazawa, T. & Ohta, S., Sintering and mechanical properties of stoichiometric mullite. *J. Am. Ceram. Soc.*, **68** (1985) C6–7.
3. Claussen, N. & Jahn, J., Mechanical properties of sintered *in situ*-reacted mullite/ $\text{ZrO}_2$  composites. *J. Am. Ceram. Soc.*, **63** (1980) 229.
4. Wei, G. C. & Becher, P. F., Development of SiC-whisker-reinforced ceramics. *Am. Ceram. Soc. Bull.*, **64** (1985) 298–304.
5. Liu, H. Y., Claussen, N., Hoffmann, M. J. & Petzow, G., Fracture sources and processing improvements of SiC-whisker-reinforced mullite ( $\text{ZrO}_2$ ) composites. *J. Eur. Ceram. Soc.*, **7** (1991) 41–7.
6. Nischik, C., Seibold, M., Travitzky, N. A & Claussen, N., Effect of processing on mechanical properties of platelet-reinforced mullite composites. *J. Am. Ceram. Soc.*, **74** (1991) 2464–8.
7. Niihara, K., New design concept of structural ceramics–ceramic nanocomposites. *J. Ceram. Soc. Japan, Int. Ed.*, **99** (1991) 945–52.
8. Wu, S., Holz, D. & Claussen, N., Mechanisms and kinetics of reaction-bonding  $\text{Al}_2\text{O}_3$  (RBAO) ceramics. *J. Am. Ceram. Soc.*, **76** (1993) 970–80.
9. Holz, D., Wu, S., Scheppokat, S. & Claussen, N., Effect of processing parameters on phase and microstructure evolution in RBAO ceramics. *J. Am. Ceram. Soc.*, **77** (1994) 2509–17.
10. Claussen, N., Wu, S. & Holz, D., Reaction bonding of aluminum oxide (RBAO) composites: Processing, reaction mechanisms, and properties. *J. Eur. Ceram. Soc.*, **14** (1994) 97–109.
11. Wu, S. & Claussen, N., Fabrication and properties of low-shrinkage reaction-bonded mullite. *J. Am. Ceram. Soc.*, **74** (1991) 2460–3.
12. Wu, S. & Claussen, N., Reaction bonding and mechanical properties of Mullite/SiC composites. *J. Am. Ceram. Soc.*, **77** (1994) 2898–904.
13. Brandt, J. & Lundberg, R., Processing of mullite-based long-fiber composites via slurry routes and by oxidation of an Al:Si alloy powder. *J. Eur. Ceram. Soc.*, **16** (1996).
14. Nakahira, A. & Niihara, K., Sintering behaviors and consolidation process for  $\text{Al}_2\text{O}_3$ /SiC nanocomposites. *J. Ceram. Soc. Japan, Int. Ed.*, **100** (1992) 448–53.
15. Stearns, L. C., Zhao, J. & Harmer, M. P., Processing and microstructure development in  $\text{Al}_2\text{O}_3$ -SiC 'nanocomposites'. *J. Eur. Ceram. Soc.*, **10** (1992) 473–7.